hydrogen.[24] Therefore, it seems that the activation energy of the reverse proton transfer in the tautomer II of 7-HF is greater as compared with that in 7-HIF, and as a result, it becomes comparable to that of tautomer I. The ground- and excited-state proton transfer was reported in the methanol solution of 7-hydroxyquinoline in the previous paper. The activation energy of this reverse proton transfer was obtained to be 4.2 kcal mol^{-1}, which is approximately two times greater than those of 7-HIF and 7-HF (2.1 kcal mol^{-1}). The fact indicates that the ground-state tautomer is more stable than those of 7-HIF and 7-HF. The transient resonance Raman study of the actual structures of two tautomers in 7-HF is now in progress by Moore and Phillips in the Royal Institute of London.

Acknowledgment. This work was indebted to T. Adachi in the early stage of experiment. The work was supported by Grant-in-Aid for Scientific Research from the Ministry of Education, Science and Culture of Japan.

Registry No. 7-HIF, 13057-72-2; 7-MOIF, 1621-56-3.

(24) Fujiwara, Y.; Itoh, M.; Sumitani, M.; Yoshihara, K. *J. Phys. Chem.* submitted for publication.

Mixed-Valence 1',6'-Dihalobiferrocenium Cations: Counterions Micromodulating Intramolecular Electron Transfer

Teng-Yuan Dong, Takeshi Kambara,[1] and David N. Hendrickson*

Contribution from the School of Chemical Sciences, University of Illinois, Urbana, Illinois 61801. *Received February 10, 1986*

Abstract: The effects on the rate of electron transfer of replacing I_3^- by Br_2I^- in the mixed-valence compounds 1',6'-diiodobiferrocenium triiodide (**3**), 1',6'-dibromobiferrocenium triiodide (**4**), and 1',6'-dichlorobiferrocenium triiodide (**2**) are examined. Replacing I_3^- by Br_2I^- in the first two complexes leads to an appreciable decrease in the rate of electron transfer, whereas in the case of the third complex an increase in the rate is seen. The triiodide complex **3** shows a single "average-valence" ^{57}Fe Mössbauer doublet at 4.2 K; that is, the electron-transfer rate is in excess of $\sim 10^7$ s^{-1} at 4.2 K. Two doublets are seen at 4.2 K for 1',6'-diiodobiferrocenium dibromoiodate (**9**). It is necessary to heat **9** to ~80 K so that the rate exceeds $\sim 10^7$ s^{-1}. Two Mössbauer doublets are also seen at 4.2 K for 1',6'-dibromobiferrocenium dibromoiodate (**10**), whereas **4** shows one doublet. The mixed-valence complex **10** needs to be heated to ~180 K to have the rate be in excess of $\sim 10^7$ s^{-1}. Complex **2** is Mössbauer-localized up to ~340 K; however replacing the I_3^- by Br_2I^- to give **8** changes this such that **8** begins to show some Mössbauer-delocalized species at ~100 K, and at 300 K there are approximately equal amounts of Mössbauer-localized and -delocalized species present. This increase in rate by replacing I_3^- by Br_2I^- is what was seen before for biferrocenium triiodide (**1**). A qualitative model is presented to explain these anion effects on the *intra*molecular electron-transfer rate of mixed-valence biferrocenes. It is shown that the difference in response of I_3^- replacement by Br_2I^- reflects the different packing arrangements in the solid state. The occurrence of a phase transition is strongly indicated. In **1** there are stacks of mixed-valence cations, and cation–cation interactions are important. The greater electron-transfer rate in biferrocenium dibromoiodate than in biferrocenium triiodide could be a reflection of three possibilities: 1, charge oscillation between two asymmetric forms of the trihalide anion is easier in Br_2I^- than in I_3^-; 2, the Br_2I^- ion begins to move between two lattice positions at lower temperatures than the I_3^- anion; and 3, the replacement of I_3^- by Br_2I^- reduces the intrastack cation–cation interactions which lead to valence trapping. The packing arrangement in **3**, **4**, **9**, and **10** is comprised of alternating stacks of cations and anions. Unlike the situation for **1**, IR and EPR results for these complexes show that the mixed-valence cation is appreciably influenced by changing the anion. The origin of this is the appreciable in-stack interaction between the terminal atom of the trihalide anion and the iodine atom on the cyclopentadienyl ring. Thus, changing I_3^- in **3** to give the Br_2I^- salt **9** leads to an increase in the in-stack cation–anion interaction, and a higher temperature is needed for **9** to achieve an electron-transfer rate in excess of $\sim 10^7$ s^{-1}.

In the last year or two there has been considerable progress made in understanding what factors control the rate of intramolecular electron transfer in the *solid state* for mixed-valence biferrocenes[2-7] and oxo-centered trinuclear iron acetates.[7-12] The exact positioning of a counterion, a ligand, or even a solvate molecule relative to the mixed-valence complex in the solid state can have a dramatic impact on the rate of intramolecular electron transfer. When there is an onset of dynamics associated with the counterion,[4,7] ligand,[7,8] or solvate molecule,[9,11,12] this probably will influence the rate of intramolecular electron transfer. In fact, because there are interactions between molecules in the solid state, frequently changes in the rate of intramolecular electron transfer are coupled to phase transitions.[7,9,10,11]

Mixed-valence compound **2** crystallizes with half a mole of I_2. The X-ray structure[5] of this compound shows that not only is the I_3^- anion asymmetric but the I_3^- counterion sits closer to one half of the cation, the iron(III) metallocene moiety. As a result, mixed-valence compound **2** is localized on the Mössbauer time scale even at 340 K.[5,13] The ground-state double-well potential-energy surface for the mixed-valence cation in **2** is asymmetric

(1) On sabbatical leave from the Department of Engineering Physics, The University of Electro-Communications, Chofu, Tokyo 182, Japan.
(2) Dong, T-Y.; Cohn, M. J.; Hendrickson, D. N.; Pierpont, C. G. *J. Am. Chem. Soc.* **1985**, *107*, 4777.
(3) Cohn, M. J.; Dong, T.-Y.; Hendrickson, D. N.; Geib, S. J.; Rheingold, A. L. *J. Chem. Soc., Chem. Commun.* **1985**, 1095.
(4) Dong, T.-Y.; Hendrickson, D. N.; Iwai, K.; Cohn, M. J.; Rheingold, A. L.; Sano, H.; Motoyama, I.; Nakashima, S. *J. Am. Chem. Soc.* **1985**, *107*, 7996.
(5) Dong, T.-Y.; Hendrickson, D. N.; Pierpont, C. G.; Moore, M. F. *J. Am. Chem. Soc.* **1986**, *108*, 963.
(6) Moore, M. F.; Wilson, S. R.; Cohn, M. J.; Dong, T.-Y.; Mueller-Westerhoff, U. T.; Hendrickson, D. N. *Inorg. Chem.* **1985**, *24*, 4559.
(7) Hendrickson, D. N.; Oh, S. M.; Dong, T.-Y.; Kambara, T.; Cohn, M. J.; Moore, M. F. *Comm. Inorg. Chem.* **1985**, *4*, 329.
(8) (a) Oh, S. M.; Hendrickson, D. N.; Hassett, K. L.; Davis, R. E. *J. Am. Chem. Soc.* **1984**, *106*, 7984. (b) Oh, S. M.; Hendrickson, D. N.; Hassett, K. L.; Davis, R. E. *J. Am. Chem. Soc.* **1985**, *107*, 8009.
(9) Oh, S. M.; Kambara, T.; Hendrickson, D. N.; Sorai, M.; Kaji, K.; Woehler, S. E; Wittebort, R. J. *J. Am. Chem. Soc.* **1985**, *107*, 5540.
(10) Kambara, T.; Hendrickson, D. N.; Sorai, M.; Oh, S. M. *J. Chem. Phys.*, in press.
(11) Sorai, M.; Kaji, M.; Hendrickson, D. N.; Oh, S. M. *J. Am. Chem. Soc.* **1986**, *108*, 702.
(12) Woehler, S. E.; Wittebort, R. J.; Oh, S. M.; Hendrickson, D. N.; Inniss, D.; Strouse, C. E. *J. Am. Chem. Soc.* **1986**, *108*, 2938.
(13) Motoyama, I.; Suto, K.; Katada, M.; Sano, H. *Chem. Lett.* **1983**, 1215.

0002-7863/86/1508-5857$01.50/0

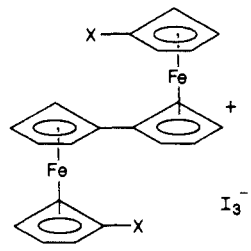

1, X = H 3, X = I
2, X = Cl 4, X = Br

due to the asymmetric environment about the cation. Intramolecular electron transfer is slow (rate $< 10^7$ s^{-1} at 340 K). On the other hand, the X-ray structure[5] for compound **3** shows that the mixed-valence cation in this compound has a symmetric environment, i.e., the two metallocene moieties in the cation are crystallographically equivalent. However, infrared data for **3** and isostructural **4** clearly indicate that the mixed-valence cations in these two compounds do have potential-energy barriers for electron transfer.[5] It is quite intriguing that the rate of intramolecular electron transfer in **3** (and **4**) exceeds the Mössbauer time scale (rate $> 10^7$ s^{-1}) at 4.2 K.[5,13,14] Obviously there is little thermal energy at 4.2 K, which implies that there is relatively rapid electron and nuclear tunneling possible, which facilitate the electron transfer between the two iron ions separated by 5.1 Å (the cation has a trans conformation in all four compounds).

At room temperature biferrocenium triiodide, **1**, shows two doublets (Fe^{II} and Fe^{III}) in a Mössbauer spectrum.[14] At temperatures above 300 K, the Mössbauer spectrum of **1** does change to eventually become a single average-valence doublet at ~357 K.[3,4] Heat capacity measurements have shown that a phase transition is involved.[15] It is likely that an order–disorder phase transition is involved, where at low temperatures electronically localized mixed-valence biferrocenium cations are ordered throughout a crystallite. The I_3^- anions are also probably asymmetric (two different I–I bond lengths) and ordered throughout the lattice. The phase transition could involve the onset of charge oscillation in the I_3^- anions which changes the ground-state double-well potential-energy surface for the mixed-valence cation from asymmetric to symmetric. This type of change would dramatically increase the rate of intramolecular electron transfer in the mixed-valence cation.

The importance of the counterion in controlling the rate of intramolecular electron transfer in **1** was very recently[3] demonstrated. We found that replacing the I_3^- by the linear Br_2I^- anion leads to a dramatic reduction by ~150 deg in the temperature where the mixed-valence biferrocenium cation is involved in intramolecular electron transfer faster than the Mössbauer technique can sense. A qualitative model has been presented[16] to explain the effects of replacing I_3^- in **1** by Br_2I^- and I_2Br^-. The importance of the cation–cation and cation–anion interactions, as well as the intrinsic charge-oscillation barrier heights in the mixed-valence cations and anions, was delineated, as they impact on the order–disorder phase transition in the biferrocenium salts.

In this paper the effect of replacing the I_3^- anion of **3** and **4** by Br_2I^- is examined. It will be seen that this replacement has the opposite effect on the rate of intramolecular electron transfer than what is seen in the case of compound **1**. An explanation for this difference is advanced, which keys on the different packing arrangements in the mixed-valence compounds.

Experimental Section

Compound Preparation. Samples of 1′,6′-dichlorobiferrocene (**5**), 1′,6′-diiodobiferrocene (**6**), and 1′,6′-dibromobiferrocene (7) were prepared and characterized as described previously.[5]

Samples of the Br_2I^- salts of **5**, **6**, and 7 were prepared by dissolving the 1′,6′-dihalobiferrocene and a stoichiometric amount of *p*-benzoquinone in hexane–benzene (1:2) at 0 °C. To this solution a stoichiometric amount of 0.1 M HBr_2I–methanol solution was added dropwise with rapid stirring. The resulting microcrystalline solid was filtered, washed with a little cold benzene, and vacuum-dried. Anal. Calcd for 1′,6′-diiodobiferrocenium dibromoiodate ($C_{20}H_{16}Fe_2I_3Br_2$): C, 26.44; H, 1.78; Fe, 12.29. Found: C, 27.02; H, 2.00; Fe, 12.30. Anal. Calcd for 1′,6′-dibromobiferrocenium dibromoiodate ($C_{20}H_{16}Fe_2Br_4I$): C, 29.49; H, 1.98; Fe, 13.71. Found: C, 29.84; H, 2.19; Fe, 13.90. Anal. Calcd for 1′,6′-dichlorobiferrocenium dibromoiodate ($C_{20}H_{16}Fe_2Cl_2Br_2I$): C, 33.10; H, 2.22; Fe, 15.39. Found: C, 32.66; H, 2.24; Fe, 15.14.

Physical Methods. ^{57}Fe Mössbauer measurements were made on a constant-acceleration instrument which has been described previously.[17] Mössbauer spectra were least-squares-fit to Lorentzian line shapes with a previously documented computer program.[18] An attempt was made to report isomer shift data relative to that of iron foil at 300 K; however, second-order Doppler effects could only be estimated due to source temperature variability (the source was located within the exchange-gas cooled cryostat). It should be noted that the isomer shifts illustrated in the figures are plotted as experimentally obtained; tabulated data should be consulted.

Variable-temperature X-band EPR spectra of powdered samples were run on a Bruker ER200 spectrometer equipped with an Oxford Instruments temperature controller. A calibrated copper–constantan thermocouple was used to determine the sample temperature. Samples were sealed in quartz tubes which had been pumped on a glass vacuum line.

Infrared spectra were obtained with a Nicolet Model MX-5 spectrometer. All samples were prepared as 13-mm KBr pellets with 2–5 mg of compound mixed well with 150 mg of KBr.

X-ray powder diffraction patterns were obtained on a Norelco (Phillips Electronics Co.) powder diffractometer equipped with a copper X-ray tube and a graphite monochromator. A computer program was used to simulate powder patterns.[19]

Results and Discussion

Compound Preparation and Structure. Microcrystalline samples, which microscopic examination showed to be single phases, of mixed-valence compounds **8**, **9**, and **10** were prepared by the

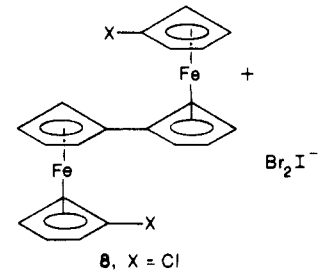

8, X = Cl
9, X = I
10, X = Br

oxidation of the 1′,6′-dihalobiferrocene by *p*-benzoquinone in solution in the presence of HBr_2I. After several attempts to grow X-ray quality crystals of these compounds by a variety of procedures, it was concluded that it is not easily done. It seems that the main problem stems from the fact that if a biferrocenium species is left in contact with the Br_2I^- ion in solution for any period of time, there is decomposition of the cation. For example, in the case of biferrocenium dibromoiodate, attempts to grow crystals by diffusing hexane into a CH_2Cl_2 solution give mostly an amorphous powder with a few crystals. An X-ray structure[20] of the crystals shows that they are biferrocenium tetrabromoferrate. Apparently, Br_2I^- in solution dissociates to give IBr which attacks the biferrocenium cation to give $FeBr_4^-$. Regardless of what actually happens, even low-temperature approaches have failed to give X-ray quality crystals of **8**, **9**, and **10**.

(14) Morrison, W. H., Jr.; Hendrickson, D. N. *Inorg. Chem.* **1975**, *14*, 2331.
(15) Sorai, M.; Nishimori, A.; Dong, T.-Y.; Cohn, M. J.; Hendrickson, D. N., submitted for publication.
(16) Dong, T-Y.; Kambara, T.; Hendrickson, D. N. *J. Am. Chem. Soc.* **1986**, *108*, 4423.
(17) Cohn, M. J.; Timken, M. D.; Hendrickson, D. N. *J. Am. Chem. Soc.* **1984**, *106*, 6683.
(18) Chrisman, B. L.; Tumolillo, T. A. *Comput. Phys. Commun.* **1971**, *2*, 322.
(19) Yvon, K.; Jeitschiko, W.; Parthe, E. *J. Appl. Crystallogr.* **1977**, *10*, 73.
(20) Geib, S. J.; Rheingold, A. L.; Dong, T.-Y.; Hendrickson, D. N. *J. Organomet. Chem.*, in press.

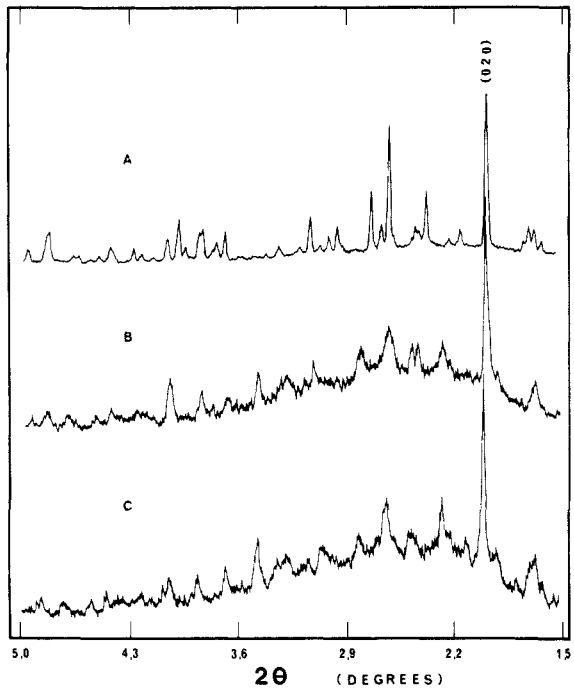

Figure 1. Room-temperature powder X-ray diffraction patterns for (A) 1',6'-diiodobiferrocenium triiodide, **3**, (B) 1',6'-diiodobiferrocenium dibromoiodate, **9**, and (C) 1',6'-dibromobiferrocenium dibromoiodate, **10**.

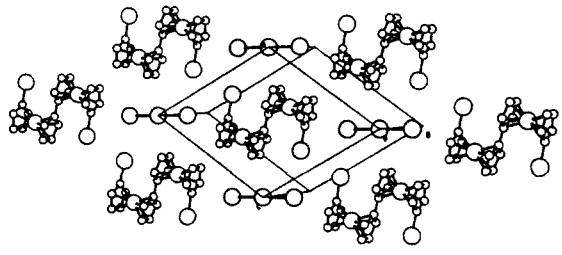

Figure 2. Pluto plot showing for compound **3** the arrangement of the 1',6'-diiodobiferrocenium cations and triiodide anions on the crystallographic mirror plane of the unit cell.

In order to determine the solid-state structure of the three new mixed-valence Br_2I^- salts, powder X-ray diffraction patterns were run at 300 K for **2–4** and **8–10**. The powder X-ray patterns for **9** and **10** are compared in Figure 1 with that for 1',6'-diiodobiferrocenium triiodide, **3**, for which a single-crystal X-ray structure is available.[3,4] The packing arrangement in **3** consists of planar layers of cations and anions that are arranged in an alternating fashion on the crystallographic *ac* mirror plane. A view of one plane of **3** is shown in Figure 2.

From Figure 1 it is clear that the triiodide salt of 1',6'-diiodobiferrocenium (**3**) diffracts better than the dibromoiodate salt (**9**) of the same cation. The Br–I–Br$^-$ anion is linear and approximately 7–10% shorter than the linear I_3^- anion. From the packing arrangement of **3** illustrated in Figure 2, it is expected that the cell parameter *b* would not vary appreciably by replacing I_3^- with Br_2I^-. A computer simulation of the powder pattern of **3** from the known unit cell parameters (space group $C2/m$) and atomic positional parameters shows that the strong powder pattern line at $2\theta = 19.9°$ is assignable to (0,2,0). It can be seen that the powder patterns for the Br_2I^- salts **9** and **10** also exhibit this strong peak. This suggests that the unit cell parameters *b*, α, and γ do not vary appreciably as a result of replacing the I_3^- anion with the Br_2I^- anion in the 1',6'-diiodobiferrocenium and 1',6'-dibromobiferrocenium salts. The shifting of the powder pattern lines at higher 2θ values is likely due to a compression along the cation–anion column for the shorter Br_2I^- anion. It is probable that **9** and **10** are isostructural with **3**.

From a comparison of the X-ray powder patterns of structurally characterized[5] $[(\eta^5\text{-}C_5ClH_4)_2Fe_2(\eta^{10}\text{-}C_{10}H_8)]I_3\cdot{}^1/_2I_2$ and the analogous Br_2I^- salt **8**, it is clear that these two complexes are *not* isostructural (figure available in supplementary material). This is not surprising in view of the fact that compound **2** has "extra" I_2 in the lattice, whereas, the microanalysis of compound **8** does *not* indicate such extra halogen content.

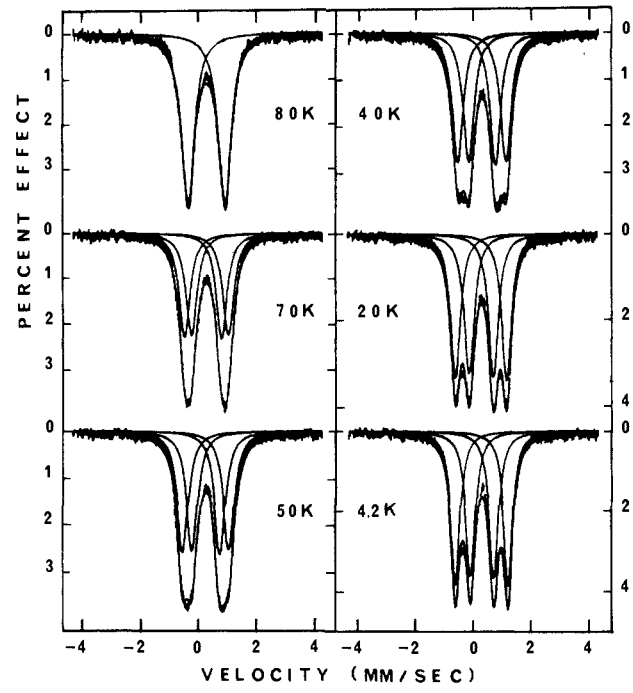

Figure 3. Variable-temperature ^{57}Fe Mössbauer spectra of 1',6'-diiodobiferrocenium dibromoiodate, **9**.

^{57}Fe Mössbauer Spectroscopy. Relative to the triiodide salts **2–4**, the mixed-valence Br_2I^- salts **8–10** exhibit interesting Mössbauer characteristics. The variable-temperature ^{57}Fe Mössbauer spectra of mixed-valence compound **9** are illustrated in Figure 3. At 4.2 K two quadrupole-split doublets can be seen, one characteristic of a iron(II) metallocene with a quadrupole splitting of $\Delta E_Q = 1.821$ (3) mm/s and the other characteristic of a iron(III) metallocene with $\Delta E_Q = 0.805$ (3) mm/s. Both doublets have the same area as deduced by a least-squares fitting with Lorentzian line shapes. Mössbauer fitting parameters are collected in Table I. It is interesting that the Br_2I^- salt **9** transfers electrons slower than the Mössbauer time scale at 4.2 K, whereas the triiodide **3** shows only a single doublet at 4.2 K. As can be seen in Figure 3, increasing the temperature of **9** above 4.2 K leads to the two doublets moving together to become a single "average-valence" doublet at 80 K. At this temperature the intramolecular electron-transfer rate is greater than $\sim 10^7$ s^{-1}. The fact that the single doublet seen at 80 K does correspond to an average signal is substantiated by the $\Delta E_Q = 1.272$ (3) mm/s value, which is close to the average of 1.315 mm/s for the two doublets in the 4.2 K spectrum. Three additional points need to be made about the Mössbauer data for **9**. First, increasing the temperature above 80 K leads to no further spectral changes (see Table I); the single doublet persists. Second, at all temperatures from 4.2 to 80 K, the spectrum can be fit with only two doublets. Finally, there is no line broadening evident in the spectra taken at temperatures between 4.2 and 80 K. This same type of absence of line broadening in spite of the presence of an averaging process has been noted[4,21] for four 1',6'-dialkylbiferrocenium triiodides, where the alkyl substituents includes ethyl, *n*-propyl, *n*-butyl, and benzyl. These four compounds exhibit their temperature dependencies in the range of $\sim$200 to $\sim$280 K.

The Mössbauer characteristics of **10** are somewhat different; see Figure 4. Two equal-area doublets can be seen in the 4.2 K spectrum of **10**, one with $\Delta E_Q = 1.930$ (6) mm/s and the other

(21) Iijima, S.; Saida, R.; Motoyama, I.; Sano, H. *Bull. Chem. Soc. Jpn.* **1981**, *54*, 1375.

Table I. ^{57}Fe Mössbauer Least-Squares Fitting Parameters[a]

compound	T, K	ΔE_Q, mm/s	δ, mm/s	Γ,[b] mm/s		% del; % loc
1′,6′-diiodobiferrocenium dibromoiodate	270	1.263 (3)	0.494 (1)	0.386 (5)	0.364 (4)	
	105	1.263 (3)	0.520 (1)	0.498 (2)	0.492 (4)	
	80	1.272 (3)	0.518 (2)	0.530 (6)	0.526 (6)	
	70	1.514 (6)	0.520 (3)	0.450 (9)	0.460 (10)	
		1.043 (6)	0.525 (3)	0.458 (9)	0.442 (9)	
	60	1.552 (5)	0.517 (3)	0.456 (9)	0.470 (9)	
		1.003 (6)	0.529 (3)	0.466 (8)	0.456 (8)	
	50	1.597 (5)	0.519 (2)	0.448 (4)	0.460 (4)	
		0.965 (5)	0.527 (2)	0.454 (4)	0.440 (4)	
	40	1.663 (5)	0.521 (2)	0.438 (4)	0.442 (4)	
		0.923 (4)	0.529 (2)	0.440 (4)	0.430 (4)	
	20	1.766 (4)	0.523 (2)	0.404 (3)	0.396 (3)	
		0.836 (4)	0.533 (2)	0.416 (3)	0.406 (3)	
	4.2	1.821 (3)	0.519 (2)	0.364 (4)	0.362 (4)	
		0.805 (3)	0.532 (3)	0.386 (5)	0.380 (2)	
1′,6′-dibromobiferrocenium dibromoiodate	270	1.222 (4)	0.520 (2)	0.478 (8)	0.440 (6)	100; 0
	200	1.244 (3)	0.519 (2)	0.534 (6)	0.494 (6)	100; 0
	180	1.254 (4)	0.519 (2)	0.552 (6)	0.524 (6)	100; 0
	160	1.816 (58)	0.516 (29)	0.374 (82)	0.396 (82)	70.4; 19.6
		1.248 (5)	0.519 (3)	0.442 (55)	0.432 (51)	
		0.767 (44)	0.534 (22)	0.428 (65)	0.384 (61)	
	140	1.825 (52)	0.516 (26)	0.414 (63)	0.410 (65)	61.2; 38.8
		1.256 (6)	0.520 (3)	0.438 (62)	0.434 (57)	
		0.783 (39)	0.535 (20)	0.460 (46)	0.406 (47)	
	120	1.824 (45)	0.525 (22)	0.428 (48)	0.426 (50)	50.0; 50.0
		1.262 (7)	0.522 (3)	0.428 (72)	0.412 (71)	
		0.790 (33)	0.527 (17)	0.438 (37)	0.408 (35)	
	100	1.810 (28)	0.508 (14)	0.396 (36)	0.408 (34)	43.0; 57.0
		1.253 (6)	0.517 (3)	0.422 (72)	0.416 (74)	
		0.766 (23)	0.523 (11)	0.424 (27)	0.390 (27)	
	75	1.831 (20)	0.508 (10)	0.400 (22)	0.402 (21)	29.4; 70.6
		1.276 (8)	0.513 (4)	0.402 (79)	0.384 (75)	
		0.749 (19)	0.518 (9)	0.408 (20)	0.400 (19)	
	50	1.867 (12)	0.507 (6)	0.374 (15)	0.382 (16)	20.8; 79.4
		1.286 (11)	0.506 (6)	0.390 (86)	0.400 (84)	
		0.721 (12)	0.509 (6)	0.400 (14)	0.384 (14)	
	30	1.908 (7)	0.509 (4)	0.342 (11)	0.342 (12)	16.8; 83.2
		1.283 (11)	0.501 (6)	0.420 (9)	0.414 (8)	
		0.685 (8)	0.524 (4)	0.370 (12)	0.356 (10)	
	4.2	1.930 (3)	0.513 (1)	0.352 (4)	0.360 (4)	0.0; 100
		0.700 (3)	0.527 (1)	0.400 (5)	0.374 (4)	
1′,6′-dichlorobiferrocenium dibromoiodate	300	1.867 (12)	0.479 (6)	0.372 (32)	0.342 (30)	52.4; 47.6
		1.208 (8)	0.490 (4)	0.590 (64)	0.596 (63)	
		0.556 (10)	0.488 (5)	0.352 (24)	0.338 (25)	
	270	1.896 (7)	0.488 (3)	0.322 (21)	0.324 (20)	46.8; 53.2
		1.197 (8)	0.503 (4)	0.582 (59)	0.596 (54)	
		0.548 (7)	0.496 (3)	0.320 (18)	0.324 (18)	
	240	1.952 (6)	0.495 (3)	0.338 (13)	0.326 (13)	30.2; 69.8
		1.210 (9)	0.493 (5)	0.526 (68)	0.554 (67)	
		0.531 (5)	0.502 (3)	0.332 (11)	0.358 (11)	
	200	2.017 (3)	0.500 (2)	0.308 (8)	0.302 (8)	22.2; 77.8
		1.255 (11)	0.513 (6)	0.564 (73)	0.548 (71)	
		0.505 (4)	0.509 (2)	0.340 (8)	0.344 (8)	
	160	2.068 (2)	0.505 (1)	0.284 (5)	0.284 (5)	16.3; 83.4
		1.320 (14)	0.526 (7)	0.548 (77)	0.610 (78)	
		0.490 (3)	0.519 (2)	0.330 (6)	0.336 (6)	
	120	2.101 (2)	0.509 (1)	0.278 (4)	0.282 (4)	10.2; 89.8
		1.382 (21)	0.545 (11)	0.524 (92)	0.612 (96)	
		0.471 (2)	0.524 (1)	0.318 (4)	0.322 (4)	
	100	2.110 (2)	0.511 (1)	0.274 (3)	0.280 (3)	6.8; 93.2
		1.404 (27)	0.544 (13)	0.478 (104)	0.552 (109)	
		0.470 (2)	0.528 (1)	0.308 (4)	0.310 (4)	
	4.2	2.169 (2)	0.514 (1)	0.308 (3)	0.316 (3)	0.0; 100
		0.443 (2)	0.514 (1)	0.318 (3)	0.370 (4)	

[a] The estimated standard deviations in the least-significant figures are given in parentheses. [b] Full width at half-height taken from the least-squares fitting program. The width for the line at more negative velocity is listed first for each doublet.

with ΔE_Q = 0.700 (3) mm/s. As the temperature of **10** is increased, a third doublet with ΔE_Q = 1.28 mm/s can be seen. This third doublet is clearly visible in the 75 and 100 K spectra, even without computer fitting. Thus, increasing the temperature of **10** above 4.2 K leads to an increase in the relative intensity of the third doublet at the expense of the Fe^{II} and Fe^{III} doublets. Table I gives the fitting parameters, which indicate that there are equal amounts of "localized" and "delocalized" signals at 120 K. At temperatures of 180 K or higher, only the "delocalized" doublet is seen.

The increase in intramolecular electron-transfer rate resulting from replacing I_3^- by Br_2I^- in **1** is also seen for the 1′,6′-dichlorobiferrocenium cation. In Figure 5 are shown variable-temperature Mössbauer spectra for the Br_2I^- salt **8**. Least-squares fitting parameters are given in Table I. Two equal-area doublets can be seen in the 4.2 K spectrum, one with ΔE_Q = 2.169 (2)

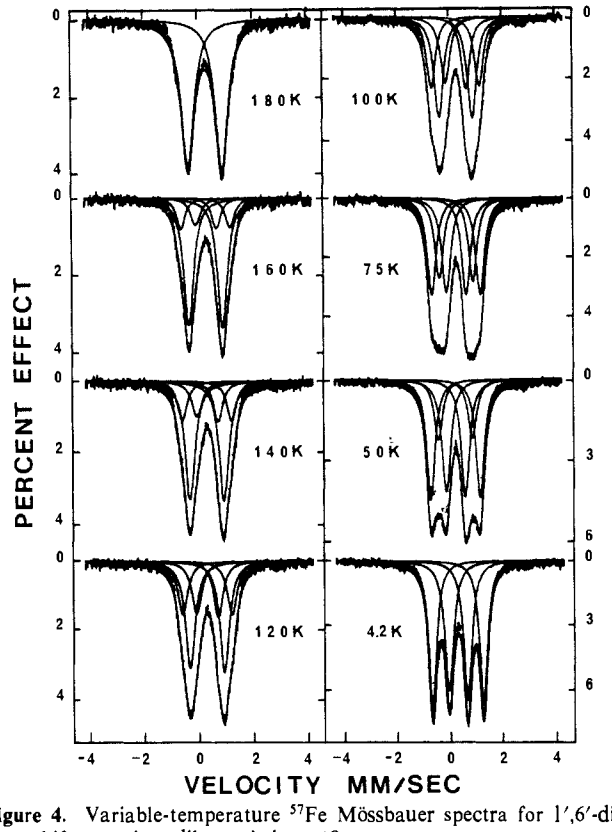

Figure 4. Variable-temperature ^{57}Fe Mössbauer spectra for 1',6'-dibromobiferrocenium dibromoiodate, **10**.

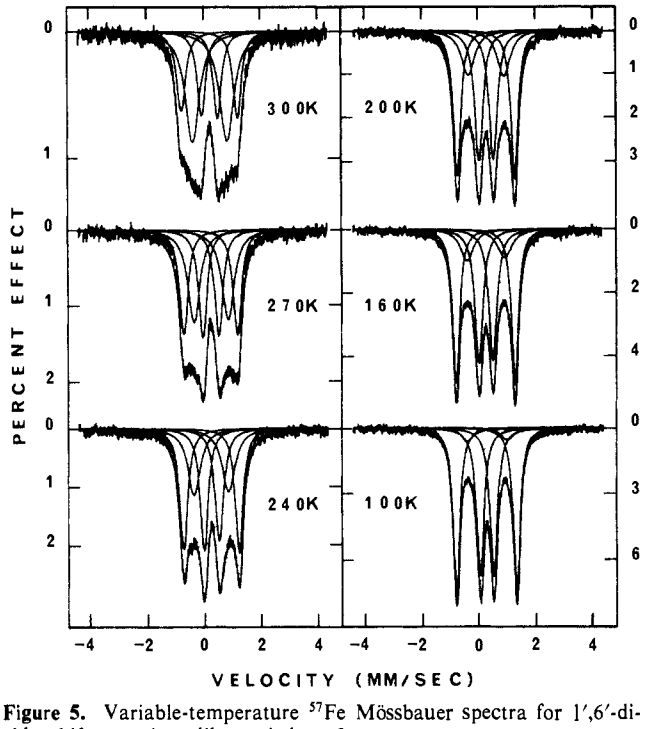

Figure 5. Variable-temperature ^{57}Fe Mössbauer spectra for 1',6'-dichlorobiferrocenium dibromoiodate, **8**.

mm/s and the other with ΔE_Q = 0.443 (2) mm/s. It should be noted that the ΔE_Q value for the Fe^{II} site is appreciably larger and the Fe^{III} ΔE_Q value smaller than the values extracted from the 4.2 K spectra of **9** and **10**. It is clear that as the rate of some averaging process (vide infra) becomes comparable to the inverse of the Mössbauer time scale, the ΔE_Q value for the "Fe^{II}" signal will begin to decrease, whereas the ΔE_Q value for the "Fe^{III}" signal will begin to increase. Thus, it is clear that **9** and **10** are experiencing some dynamical process even at 4.2 K that is *effectively* increasing the intramolecular electron-transfer rate so that it is

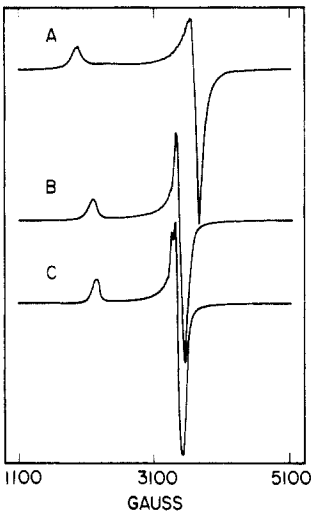

Figure 6. X-band EPR spectra at 4.2 K of polycrystalline samples of (A) 1',6'-dichlorobiferrocenium dibromoiodate, (B) 1',6'-dibromobiferrocenium dibromoiodate, and (C) 1',6'-diiodobiferrocenium dibromoiodate.

on the Möessbauer time scale. If this is the case, then it can be concluded that at least at these low temperatures there is an appreciable rate of tunneling in these complexes, for there is obviously little thermal energy available at 4.2 K.

As is summarized in Table I and shown in Figure 5, above 100 K a third "delocalized" doublet with ΔE_Q = 1.3 mm/s can be seen in the Mössbauer spectra of **8**. An appreciable increase in the amount of this third doublet can be seen with increasing sample temperature. The 300 K spectrum shows approximately equal amounts of the "delocalized" and "localized" signals. Unfortunately, the Br_2I^- salt **8** decomposes at temperatures above ~300 K. It is evident that the temperature dependence of the Mössbauer spectrum of **8** is similar to that of **10**; however, a much larger range of temperature is needed for the complete conversion from localized to delocalized for **8**.

Electron Paramagnetic Resonance. As discussed in detail in a previous paper,[5] EPR is a useful tool in studying mixed-valence biferrocenes. In summary, a mixed-valence biferrocene species which is electronically localized will possess appreciable g-tensor anisotropy, $\Delta g = g_\parallel - g_\perp$. Ferrocenium triiodide[22] gives an EPR signal at 20 K characterized by $g_\parallel$ = 4.35 and $g_\perp$ = 1.26 (Δg = 3.09). At 12 K biferrocenium triiodide[14] has $g_\parallel$ = 3.58 and $g_\perp$ = 1.72 with Δg = 1.86. The reduction in Δg in going from ferrocenium triiodide to biferrocenium triiodide largely reflects the reduced crystal field symmetry at the Fe^{III} ion of the biferrocenium cation relative to that of the Fe^{III} ion in the ferrocenium salt.[5,23] Mixed-valence biferrocenes that have delocalized electron structures where there is *no* potential-energy barrier for electron transfer have considerably reduced Δg values. For example, the I_3^- salt of the mixed-valence bis(fulvalene) diiron cation gives a rhombic EPR spectrum with g values of 2.52, 1.97, and 1.88 (Δg = 0.60).[14]

X-band EPR spectra were run at 4.2 K for microcrystalline samples of **8**–**10**. As can be seen in Figure 6, an axial-type spectrum is seen for **8** and **10**, whereas the diiodo compound **9** shows some splitting in the $g_\perp$ signal. The g values calculated from the spectra in Figure 6 are collected in Table II together with data for the analogous mixed-valence triiodide salts.

There is one very intriguing observation that can be made about the data in Table II. Whereas replacing I_3^- by Br_2I^- in biferrocenium triiodide does *not* appreciably affect the EPR signal (see Table II), there is an appreciable difference in the EPR signals of triiodide **3** and dibromoiodide **9** (also between **4** and **10**). For the 1',6'-diiodobiferrocenium salts, $g_\parallel$ changes from 2.75 to 3.02

(22) (a) Anderson, S. E.; Rai, R. *Chem. Phys.* **1973**, *2*, 216; (b) Sohn, Y. S.; Hendrickson, D. N.; Gray, H. B. *J. Am. Chem. Soc.* **1971**, *93*, 3603.
(23) Duggan, D. M.; Hendrickson, D. N. *Inorg. Chem.* **1975**, *14*, 955.

Table II. Electron Paramagnetic Resonance Data[a]

compd	T, K	$g_{\parallel}$	$g_{\perp}$	Δg^b
I[c]	12	3.58	1.72	1.86
biferrocenium dibromoiodate	4.2	3.60	1.75	1.85
2[d]	4.2	3.28	1.88	1.40
3[d]	4.2	2.75	2.01	0.76
4[d]	4.2	2.76	2.01	0.78
			1.96	
8	4.2	3.43	1.82	1.61
9	4.2	3.02	2.01	1.04
			1.96	
10	4.2	3.08	1.94	1.14

[a] EPR spectra were run for microcrystalline samples. [b] This is the g-tensor anisotropy defined as $\Delta g = g_{\parallel} - g_{\perp}$. When a rhombic signal is seen, an average of the "perpendicular" signals is used for $g_{\perp}$. [c] Sohn, Y. S.; Hendrickson, D. N.; Gray, H. B. *J. Am. Chem. Soc.* **1971**, *93*, 3603. [d] See ref 5.

with much smaller changes in $g_{\perp}$ as the counterion is changed from I_3^- to Br_2I^-. In short, the counterion has a dramatic impact on the EPR characteristics of the mixed-valence 1′,6′-diiodobiferrocenium and 1′,6′-dibromobiferrocenium salts. The reason for this will become clear in later sections of this paper. It is clear, however, that regardless of the origin of the effect, the mixed-valence diiodo and dibromo cations are appreciably different in the two lattices. It may be that in the I_3^- lattices these two cations are not only involved effectively in intramolecular electron transfer at a rate that exceeds the ^{57}Fe Mössbauer time scale but also is faster than the EPR time scale (rate faster than $\sim 10^9$–10^{10} s^{-1}). The former is a certainty; the latter is only probable. Single-crystal EPR studies are needed. In the Br_2I^- salts **9** and **10** the cations may be transferring electrons slower than the EPR time scale.

Variable-temperature EPR spectra were also run for the Br_2I^- salts **8**–**10**. The EPR signals for these compounds are visible at low temperatures but cannot be seen at temperatures above ~150 K. In other words, the $g_{\parallel}$ and $g_{\perp}$ signals in a given spectrum broaden with increasing temperature without changing magnetic field position. Eventually the spin–lattice relaxation is so fast that these signals cannot be seen.

Infrared Spectroscopy. IR spectroscopy should be useful in determining whether the electron-transfer rate in a given mixed valence compound is greater than or less than $\sim 10^{12}$ s^{-1}. IR data potentially could also be useful in elucidating the nature of the environmental perturbation of a mixed-valence species. It has been shown that the cyclopentadienyl perpendicular C–H bending is most diagnostic of the oxidation of iron metallocenes.[24] This band is seen at 815 cm^{-1} for ferrocene and at 851 cm^{-1} for ferrocenium triiodide.

FTIR spectra were run at room temperature for KBr pellets of the Br_2I^- salts **8**–**10**; see Figure 7. Band positions for the perpendicular C–H bending and asymmetric ring–metal–ring stretching vibrations are listed in Table III for these three Br_2I^- salts as well as for the corresponding I_3^- salts. The mixed-valence compound **9** shows relatively strong bands at 843 and 820 cm^{-1}. It is clear that on the IR time scale ($\sim 10^{-12}$ s) **9** has both Fe^{III} and Fe^{II} moieties. Similar conclusions can be made from the IR spectra of mixed-valence **8** and **10**. Furthermore, it is interesting to note that in terms of the cyclopentadienyl C–H perpendicular bending vibrations, there is little difference between the Br_2I^- and I_3^- salts of a given mixed-valence cation; see Table III. This is important for it substantiates the view we previously advanced[5] that compounds **3** and **4** do have potential-energy barriers for electron transfer, even though they transfer electrons faster than the Mössbauer time scale at 4.2 K.

The most revealing and interesting infrared data are found in the anion dependence of the asymmetric ring–metal–ring stretching vibration of the mixed-valence cation. A careful comparison of the spectra of triiodide **3** with dibromoiodide **9** shows that the only noticeable change occurs in the asymmetric ring–metal–ring stretching band which shifts from 452 cm^{-1} in **3** to 434 cm^{-1} in **9**. A similar large shift occurs in the 1′,6′-dibromobiferrocenium salts from 452 cm^{-1} for **4** to 438 cm^{-1} for **10**. On the other hand, a smaller shift *in the opposite sense* is seen for the biferrocenium cation upon changing the I_3^- counterion to Br_2I^-. The shift is from 485 to 492 cm^{-1}. Thus, the impact of changing the anion in the case of the biferrocenium cation is less than in the cases of the 1′,6′-diiodobiferrocenium and 1′,6′-dibromobiferrocenium cations. As we will discuss in detail in the next section, this difference is likely due to the difference in packing arrangements that exist in these two types of solids.

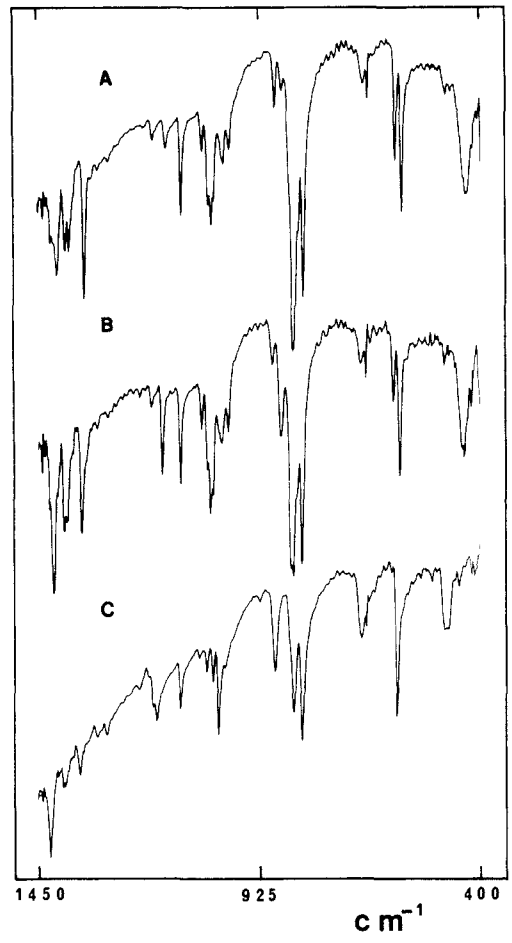

Figure 7. KBr-pellet FTIR spectra at room temperature for (A) 1′,6′-diiodobiferrocenium dibromoiodate, (B) 1′,6′-dibromobiferrocenium dibromoiodate, and (C) 1′,6′-dichlorobiferrocenium dibromoiodate.

It must be emphasized that in the above discussion the ring–metal–ring stretching mode that is described is assumed to be one of a monomeric unit, i.e., the $(\eta^5\text{-}XC_5H_4)(\eta^5\text{-}C_5H_4)Fe$ moiety. That is, it is assumed that there is only a weak coupling between vibrational modes on the two metallocene units in a mixed-valence cation. To a first approximation each $(\eta^5\text{-}C_5H_4)(\eta^5\text{-}C_5H_4)Fe$ unit is thought of as a linear Y–X–Y molecule which has a symmetric Raman-active stretching mode as well as an asymmetric IR-active stretching mode. For an XY_2 molecule the analytical expressions for the symmetric and asymmetric vibrational frequencies are given by Herzberg[25] as

$$\nu_s = \left[\frac{(k + k_{12})}{0.589M_Y}\right]^{1/2}$$

$$\nu_a = \left[\frac{(1 + 2M_Y/M_X)(k - k_{12})}{0.589M_Y}\right]^{1/2}$$

In these expressions M_Y and M_X are the masses of Y and X, k

(24) Kramer, J. A.; Hendrickson, D. N. *Inorg. Chem.* **1980**, *19*, 3330.

(25) Herzberg, G. *Infrared and Raman Spectra*; Van Nostrand: New York, 1945.

Table III. FTIR Data[a]

compd	⊥ C–H bending		asym. ring–Fe–ring stretch
	Fe^{III}	Fe^{II}	
3	845 (s)	820 (s)	452 (m); 437 (w, sh)
9	843 (s)	820 (s)	434 (m)
4	849 (s)	822 (s)	452 (m)
10	841 (s)	821 (s)	438 (m)
$2 \cdot {}^1/_2I_2$	845 (m)	822 (m)	485 (w); 473 (w)
8	841 (m)	822 (m)	480 (m, br)
1	843 (sh); 826 (m)	820 (m); 812 (sh)	485 (w); 475 (w)
biferrocenium dibromoiodate	829 (m)	815 (m)	492 (vw, br)

[a] Peak positions are given in cm^{-1} for KBr pellets.

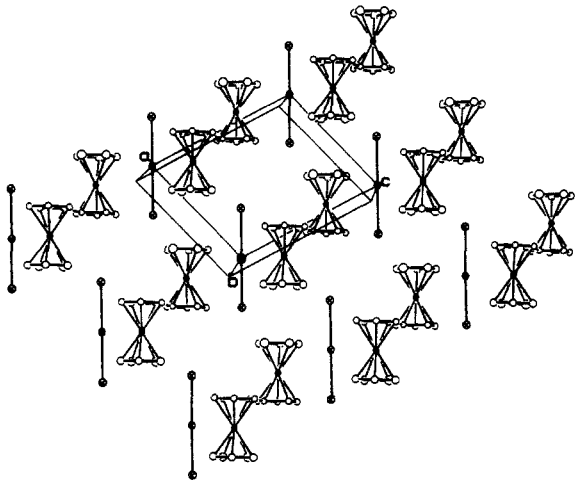

Figure 8. ORTEP plot showing the arrangement of biferrocenium cations and triiodide anions in biferrocenium triiodide as viewed down the *b* axis.

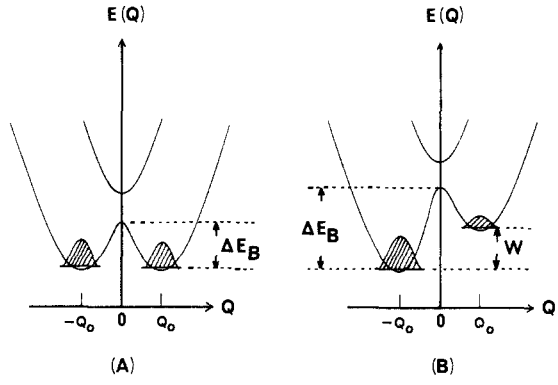

Figure 9. Potential energy plotted as a function of the out-of-plane combination of the two symmetric metal–ligand breathing vibrational modes on the two halves of a binuclear mixed-valence species. Diagram A is for a symmetric mixed-valence complex in the absence of environmental effects. Diagram B results if the environment about the binuclear mixed-valence complex is asymmetric.

is the force constant for stretching a X–Y bond, and k_{12} is the interaction force constant. Thus, when the IR-active ν_a vibration is seen to shift to lower energy in replacing the I_3^- anion of **3** to give **9**, this also means that the ν_s mode is experiencing a shift to lower energy. The force constant k is reduced in going from **3** to **9**.

Micromodulation of Rate of Intramolecular Electron Transfer. The goal in this section is to present a qualitative model to explain the pronounced influence that the anion has on the rate of *intra*molecular electron transfer in the various mixed-valence biferrocene compounds. Some of the basic facts and observations are summarized: (1) There is a phase transition in biferrocenium triiodide as indicated by heat-capacity measurements.[15] (2) Structural work[5] on **2** and **3** shows that the relative position of the anion in the solid affects the rate of electron transfer in the cation. (3) The presence of a tunneling mechanism for intramolecular electron transfer is evident in the Mössbauer data for **3** and **4** at 4.2 K. (4) Replacing I_3^- by Br_2I^- leads to a decrease in the rate of electron transfer from the 1',6'-diiobiferrocenium and 1',6'-dibromobiferrocenium cations, whereas it leads to an increase for the biferrocenium and 1',6'-dichlorobiferrocenium cations. (5) The anion has an effect on the frequency of the ring–metal–ring asymmetric stretching mode of the mixed-valence cation. (6) The solid-state packing arrangements are different for biferrocenium triiodide and 1',6'-diiodobiferrocenium triiodide. (7) The temperature dependencies of the Mössbauer spectra can taken two forms: (a) two doublets move together as the temperature is increased to become an average doublet; (b) there is a superposition of localized and delocalized signals, with the latter favored at high temperatures.

In Figures 8 and 2 are shown the solid-state packing arrangements for biferrocenium triiodide, **1**, and 1',6'-diiodobiferrocenium triiodide, **9**. As can be seen, **1** consists of slipped stacks of biferrocenium cations with an appreciable intercation interaction in the form of an intermolecular cp···cp contact with an interplanar distance of 3.4 Å. The I_3^- anions are stacked next to the cation stacks in **1**. This same type of packing arrangement is found for biferrocenium dibromoiodate and the I_3^- salts of the 1',6'-diethylbiferrocenium, 1',6'-di-*n*-propylbiferrocenium, 1',6'-di-*n*-butylbiferrocenium, and 1',6'-dibenzylbiferrocenium cations.[16,26,27]

It is evident in Figure 2 that the cations and anions in **3** lie on mirror planes of symmetry. It is probably accurate to describe the mirror plane assemblies as being comprised of one-dimensional arrays of cations and anions stacked in an alternating fashion. The most significant interaction linking ions in this stack is between end iodine atoms of the I_3^- anions and the iodocyclopentadienyl iodine atoms. This I···I distance is 3.98 Å. Compound **4** is isostructural to **3**. Thus, **3** is made up of alternating stacks of cations and anions, whereas **1** is comprised of segregated stacks of cations and anions. In both cases each mixed-valence cation has four nearest-neighbor I_3^- anions in addition to any I_3^- anions in the stack.

The environment about a given mixed-valence biferrocenium cation can be symmetric or asymmetric relative to the two iron ions in the cation. If the anions are symmetrically disposed about the cation, the ground-state double-well potential-energy surface will be symmetric as indicated in Figure 9A. In this figure the potential energy of the binuclear complex is plotted as a function of the out-of-phase combination of the two totally symmetric ring–Fe–ring stretching modes, one on each of the metallocene units. If the anions are asymmetrically disposed about the cation or there is some other environmental asymmetry, the ground-state potential-energy surface will be asymmetric as indicated in Figure 9B. There is in this case a zero-point energy difference (W) between the two vibronic states, i.e., $Fe_a^{II}Fe_b^{III}$ and $Fe_a^{III}Fe_b^{II}$. The introduction of this zero-point energy difference will increase the thermal barrier for electron transfer, and the cation will tend to be electronically localized in one vibronic state. It should also be pointed out that if the main mechanism for *intra*molecular

(26) Konno, M.; Hyodo, S.; Iijima, S. *Bull. Chem. Soc. Jpn.* **1982**, *55*, 2327.

(27) Dong, T.-Y.; Pierpont, C. G.; Hendrickson, D. N., unpublished results.

electron transfer is tunneling (electron and nuclear), then the introduction of a non-zero W will also have appreciable effects on the rate of tunneling.

The anions I_3^- and Br_2I^- could also be viewed as mixed-valence species, although this is not a conventional view of these anions. Thus, I_3^- can oscillate between two different forms, which in their limiting views can be represented as $I_A-I_B\cdots I_C^-$ and $I_A^-\cdots I_B-I_C$. That is, the two bonds lengths in I_3^- (or $Br-I-Br^-$) can be unequal. This inequality could easily result from an asymmetric environment and could give an asymmetric double-well potential-energy diagram as indicated in Figure 9B. Asymmetric[28] and symmetric[29] forms of I_3^- have been noted in X-ray structures of various compounds. When the environment about a given I_3^- anion becomes symmetric, the potential-energy diagram for charge oscillation in the I_3^- anion will be symmetric as indicated in Figure 9A.

In a later paper[30] a detailed theoretical model will be given to quantitatively describe the order–disorder, electronic localization–delocalization phase transition that is present in biferrocenium triiodide and related mixed-valence complexes. In the present paper the important factors to be considered will only be qualitatively described. In view of the above simple thoughts, the factors that are potentially important in controlling the rate of *intra*molecular electron transfer in the mixed-valence cation include (1) the effective barrier for electron transfer in the mixed-valence cation, ΔE_C; (2) the effective barrier for charge oscillation in the anion, ΔE_A; (3) the in-stack *inter*molecular interaction, E_{II}; and (4) the interaction between a mixed-valence cation and nearest-neighbor anions that are not in the same stack, E_{IO}. The relative magnitudes of these four energies compared to k_BT are obviously also important.

A qualitative description of what could be happening in the phase transition in biferrocenium triiodide can be given, followed by an explanation of why replacement of I_3^- by Br_2I^- leads to a lowering by $\sim$150 deg in the temperature at which the biferrocenium cation transfers electrons faster than the Mössbauer time scale. At low temperatures the mixed-valence biferrocenium cation in **1** probably has an asymmetric environment as a result of the in-stack cation–cation interaction (E_{II}) exceeding the available thermal energy and as a result of the anion–cation interaction (E_{IO}) due to an asymmetric charge distribution in neighboring I_3^- anions. In a crystallite there would be domains, i.e., large homogeneous regions, where the electronically localized cations and distorted anions are ordered in the same sense. As the temperature of the crystallite is increased, the thermal energy would achieve such a value that the asymmetric charge distribution in the I_3^- anion ($\Delta E_A = k_BT$) could first begin to oscillate between its two limiting forms. The onset of oscillation of charge in the I_3^- anions (or movement of the I_3^- anions between two lattice positions) would symmetrize the environment about neighboring mixed-valence cations. When $E_{II} > E_{IO}$, the mixed-valence cations in each stack still remain in the ordered electronically localized state, but the stability of the state decreases. Then the charge oscillation in the I_3^- anions modulates the electron-transer rate in the cations. If the thermal energy also exceeds E_{II}, then the mixed-valence cations could as well readily oscillate between their two vibronic states, i.e., experience rapid *intra*molecular electron transfer. Depending on the relative magnitudes of E_{II} and E_{IO}, the phase transition might be imagined to proceed by a nucleation and growth mechanism.[31] Thus, as the temperature of a crystallite is increased from low temperatures, critical-size nuclei form within the *ordered*, electronically localized domains. These critical-size nuclei consist of the minimum number of cations and anions necessary to persist in a new phase. This new phase perhaps consists of rapidly oscillating I_3^- anions and electronically localized, *disordered* cations. The preferred sites for the formation of critical-size nuclei are at defects in the crystallite. After a critical-size nucleus forms, it will then grow in size at some characteristic rate to become a minority domain in the majority (original) domain. If the boundary of the minority domain encounters a defect in the crystallite, then the activation energy for further growth of the minority domain will be increased. This duality in sensitivity to defects could explain why different preparations of a given compound can have different characteristics. There is kinetic control in the solid state with different rates for the formation of critical-size nuclei and for the growth of minority domains. Eventually as the temperature of the crystallite is increased it will be completely converted from one phase to another. The rate of intramolecular electron transfer in the mixed-valence cation will also increase with increasing temperature. Therefore, finally the system becomes the high-temperature phase which consists of mixed-valence cations which are involved in rapid *intra*molecular electron transfer.

Possible origins of the effect of replacing I_3^- by Br_2I^- in biferrocenium triiodide can now be advanced. The Br_2I^- anion could have a smaller barrier (ΔE_A) for charge oscillation than does the I_3^- anion because the Br–I bonding interaction in Br_2I^- is weaker than the I–I bonding interaction in I_3^-, and the effective mass of bond stretching vibration in Br_2I^- is smaller than that in I_3^-. Thus, in the case of biferrocenium dibromoiodate it could take less thermal energy for the onset of charge oscillation in the Br_2I^- anion than it does for anion charge oscillation in biferrocenium triiodide. If the trihalide ions are not oscillating between two distorted forms, there are two other possible origins of the anion influence on the rate of intramolecular electron transfer in the biferrocenium cation. A second possibility is that as the sample temperature is increased the whole trihalide anion begins to move between two nearby lattice positions. Mathematically this will have the same effect on the cation electron-transfer rate as charge oscillation in the trihalide anion.[30] Br_2I^- has less mass than I_3^-, and it could experience an onset of motion at a lower temperature in the two biferrocenium salts. Also, it is important to note that the I_3^- anion was found to be disordered in the X-ray structure of 1,6-di-*n*-propylbiferrocenium triiodide.[26] Changing the trihalide anion in the biferrocenium salts leads to a change in the magnitude of the cation–cation interaction. If this interaction is weaker in biferrocenium dibromoiodate than in biferrocenium triiodide, this would explain why the mixed-valence cation in the Br_2I^- salt has an electron-transfer rate in excess of $\sim 10^7$ s^{-1} at 150-deg lower temperature than observed for biferrocenium triiodide. It must be emphasized that phase transitions cannot occur in one dimension. Thus, it is not sufficient just to have cooperativity develop in each stack of biferrocenium cations as a result of intermolecular interactions. There has to be interactions between the stacks of mixed-valence cations. These interstack interactions are seemingly propagated by the anions.

The effect of replacing I_3^- by Br_2I^- for 1′,6′-diiodobiferrocenium triiodide has the opposite effect; the rate of electron transfer is reduced at a given temperature. The triiodide salt **3** transfers electrons faster than $\sim 10^7$ s^{-1} at 4.2 K, whereas with the dibromoiodate salt **9** the temperature has to be increased to $\sim$80 K before the effective electron transfer rate exceeds $\sim 10^7$ s^{-1}. From the EPR and IR data for **3** and **9** it is clear that replacing I_3^- by Br_2I^- has a pronounced effect on the physical properties of the 1′,6′-diiodobiferrocenium cation. In particular, the IR data show that the force constant for stretching the Fe–ring bond is less in the Br_2I^- salt than in the I_3^- salt. As indicated above, the results from the X-ray structure[5] of **3** show the origin of this effect. In each stack of anions and cations there is an appreciable in-

(28) (a) The I_3^- anion is asymmetric in localized 1′,6′-dichlorobiferrocenium triiodide hemi(iodine); see ref 5. (b) The I_3^- anion is asymmetric in *exo,exo*-1,12-dimethyl[1.1]ferrocenophanium triiodide; see ref 6. (c) The I_3^- anion is asymmetric in $\{[(\eta^5\text{-}C_5H_5)Fe(\eta^5\text{-}C_5H_4)]Se\}I_3\cdot I_2\cdot {}^1/_2(CH_2Cl_2)$, see: Kramer, J. A.; Herbstein, F. H.; Hendrickson, D. N. *J. Am. Chem. Soc.* **1980**, *102*, 2293. (d) Tasman, H. A.; Boswijk, K. H. *Acta Crystallogr.* **1955**, *8*, 59.

(29) (a) The I_3^- anion is symmetric in biferrocenium triiodide; see ref 3 and 4. (b) The I_3^- anion is symmetric in 1′,6′-di-*n*-propylbiferrocenium triiodide at 298 K; see ref 26. (c) Runsink, J.; Swen-Walstra, S.; Migchelsen, J. *Acta Crystallogr., Sect. B* **1972**, *B28*, 1331. (d) Soled, S.; Carpenter, G. B. *Acta Crystallogr., Sect. B* **1973**, *B29*, 2556. (e) Migchelsen, T.; Vos, A. *Acta Crystallogr.* **1967**, *23*, 796.

(30) Kambara, T.; Dong, T.-Y.; Cohn, M. J.; Hendrickson, D. N., submitted to *J. Chem. Phys.*

(31) Rao, C. N. R.; Rao, K. J. *Phase Transitions in Solids*; McGraw-Hill: New York, 1978.

teraction between the terminal atoms of the I_3^- anions and the iodine atom on the cyclopentadienyl ring of the cation. The anion Br_2I^- is only 7-10% shorter than I_3^-. Because the terminal atoms of Br_2I^- carry more net negative charge than those of I_3^-, the interaction between the terminal atoms of Br_2I^- and the iodine atom on the 1',6'-diiodobiferrocenium cation would be greater than the analogous interaction in the I_3^- salt. Thus, there is a larger in-stack cation-anion interaction in the Br_2I^- salt than in the I_3^- salt. The increased cation-anion interaction in the Br_2I^- salt effectively reduces the frequency for the ring-metal stretching vibration of the cation relative to what is in the I_3^- salt. In other words, the increased anion-cation interaction in the Br_2I^- salt **9** increases the effective mass of the iodocyclopentadienyl ligand compared to what is in the I_3^- salt **3**.

The dependence of the force constant k on the anion explains the dependence of electron localization in mixed-valence cations on anion, because the energy barrier ΔE_C in the cation increases with decreasing k.[32] (It is seen from Table III that in biferrocenium compounds the situation is the reverse, as it should be.) In short, replacing I_3^- by Br_2I^- in 1',6'-diiodobiferrocenium triiodide increases the in-stack cation-anion interaction, E_{II}, and as a consequence the energy difference W (see Figure 9B) both for cations and for anions increases. Compound **9** has to be heated to ~80 K in order to experience cation electron transferring faster than $\sim 10^7$ s^{-1}, whereas compound **3** achieves this at even 4.2 K.

This type of dependence of the energy difference W on the anion-cation interaction E_{II} also explains reasonably the dependence of electron-delocalization temperature on the substituent molecule X. The electron delocalization in **9** (X = I) occurs at lower temperature than in **10** (X = Br), because the intra-stack anion-cation interaction E_{II} is larger for **10** than for **9**. If **8** (X = Cl) has the same crystal structure as **9** and **10**, the electron delocalization in **8** should occur at higher temperature than that in **10** and **9** as it does, because the substituent Cl atom in **8** carries more net negative charge than the substituent Br and I atoms in **10** and **9**, respectively.

Acknowledgment. We are grateful for support from National Institutes of Health Grant HL13652.

Supplementary Material Available: Figure comparing powder XRD patterns for compounds **2** and **8** (1 page). Ordering information is given on any current masthead page.

(32) Wong, K. Y. Schatz, P. N. *Prog. Inorg. Chem.* **1981**, *28*, 369.

Transmembrane Electron Transfer as Catalyzed by Poly(ethylenimine)-Linked Manganese Porphyrins†

Thomas J. Dannhauser,* Mamoru Nango,‡ Naoto Oku, Kazunori Anzai, and Paul A. Loach

Contribution from the Department of Chemistry and the Department of Biochemistry, Molecular Biology, and Cell Biology, Northwestern University, Evanston, Illinois 60201.
Received November 19, 1985

Abstract: Poly(ethylenimine)-linked manganese porphyrins associate with phospholipid bilayers in a manner that allows the porphyrin to penetrate the membrane to a depth limited by the hydrocarbon spacer linking it to the extremely hydrophilic polymer. Control of the length of this spacer group and the sidedness of the incorporation of these complexes in liposome membranes permit systematic variation of the minimum distances separating two such derivatives incorporated from opposite sides of the membrane bilayer. Examination of transmembrane electron transport as catalyzed by these porphyrin complexes reveals that significant rates of electron transfer are observed only when the edge-to-edge distance separating two porphyrins is approximately 4 Å or less. Comparison to theory and relevance to biological electron transfer are discussed.

The study of electron-transfer reactions associated with biological membranes is hindered by our limited knowledge of the relative locations and orientations of the electrochemical prosthetic groups.[1-4] The use of chemical models to provide insight into possible reactions in biological systems has been a valuable tool.[5-9] In an effort to better understand electron transport in bioenergetic membranes, our laboratory and others have reported model systems in which electrons are transported across lipid bilayers. Some of the membrane-soluble electron-transfer catalysts employed in these systems are ferrocene,[10,11] quinones,[10-13] metalloporphyrins,[14,15] chlorophylls,[16] viologens,[17] ruthenium complexes,[18] and isolated cytochromes.[19] The work of Hinkle[10,11] and Hauska[12,13] showed quinones to be capable of transporting both protons and electrons across a membrane, while ferrocene was demonstrated to be an electrogenic catalyst, that is, capable of electron transport only.[10,11] Our laboratory has shown that

†This research was supported by research grants from the National Science Foundation (PCM-7816669) and the U.S. Public Health Service (GM-26098).

‡Current address: Department of Applied Chemistry, University of Osaka Prefecture, Sakai, Osaka 591, Japan.

*Current address: Department of Chemistry, University of Rochester, Rochester, New York 14620.

(1) Boyer, P. D.; Chance, B.; Ernster, L.; Mitchell, P.; Racker, E.; Slater, E. C. *Annu. Rev. Biochem.* **1977**, *46*, 955-1026.
(2) Capaldi, R. A.; Malatesta, F.; Darley-Usmar, V. M. *Biochim. Biophys. Acta* **1983**, *726*, 135-148.
(3) Hauska, G.; Hurt, E.; Gabellini, N.; Lockau, W. *Biochim. Biophys. Acta* **1983**, *726*, 97-133.
(4) Trumpower, B. L. *J. Bioenerg. Biomembr.* **1981**, *13*, 1-24.
(5) Ibers, J. A.; Holm, R. H. *Science (Washington, DC)* **1980**, *209*, 223-235.
(6) Traylor, T. G. *Acc. Chem. Res.* **1981**, *14*, 102-109.
(7) Strothkamp, K. G.; Lippard, S. J. *Acc. Chem. Res.* **1982**, *15*, 318-326.
(8) Kong, K. L. Y.; Spears, K. G.; Loach, P. A. *Photochem. Photobiol.* **1982**, *35*, 545-553.
(9) Fujita, I.; Davis, M. T.; Fajer, J. *J. Am. Chem. Soc.* **1980**, *100*, 6280-6282.
(10) Hinkle, P. *Biochem. Biophys. Res. Commun.* **1970**, *41*, 1375-1381.
(11) Hinkle, P. C. *Fed. Proc., Fed. Am. Soc. Exp. Biol.* **1973**, *32*, 1988-1992.
(12) Futami, A.; Hurt, E.; Hauska, G. *Biochim. Biophys. Acta* **1979**, *547*, 583-596.
(13) Futami, A.; Hauska, G. *Biochim. Biophys. Acta* **1979**, *547*, 597-608.

0002-7863/86/1508-5865$01.50/0